

# Channel Estimation for Reconfigurable Intelligent Surface-aided 6G NOMA Systems using CNN-based Quantum LSTM Model

Nhien Q. T. Thoong\*, Adnan A. Cheema<sup>†</sup>, Saeed R. Khosravirad<sup>‡</sup>, Octavia A. Dobre\*, Trung Q. Duong\*<sup>§</sup>

\*Faculty of Engineering and Applied Science, Memorial University, St. John's, Canada.

<sup>†</sup>School of Engineering, Ulster University, Belfast, UK.

<sup>‡</sup>Nokia Bell Labs, Murray Hill, NJ, USA.

<sup>§</sup>School of Electronics, Electrical Engineering and Computer Science, Queen's University Belfast, Belfast, UK.

Emails: {qtnthoong, odobre, tduong}@mun.ca), a.cheema@ulster.ac.uk, saeed.khosravirad@nokia-bell-labs.com

**Abstract**—With the rapid development of communication applications, the integration of reconfigurable intelligent surface (RIS) and non-orthogonal multiple access (NOMA) techniques has emerged as a promising approach to enhance connectivity and data transmission rate in future wireless networks. To successfully deploy RIS-NOMA aided 6G network, an accurate channel estimation is a crucial task. Quantum machine learning (QML) is a novel approach showing potential computational advantages in various problems of 6G wireless communications. However, its application, particularly in channel estimation, remains largely theoretical rather than adopted in practice. We propose a hybrid quantum-classical neural network model based on convolutional neural network (CNN) and quantum long short-term memory (QLSTM) for channel estimation in RIS-aided 6G NOMA system. Our results show that the proposed CNN-QLSTM model has a better channel prediction compared to its classical counterpart with regard to root mean square error (RMSE) and mean absolute error (MAE).

**Index Terms**—Channel estimation, CNN-QLSTM, QLSTM, NOMA, RIS, 6G.

## I. INTRODUCTION

The sixth-generation (6G) wireless communication networks are attracting global attention from researchers and industries with an aim to overcoming the challenges faced by the previous communication networks (e.g. 5G and xG). It is expected that 6G will significantly enhance the network performance in terms of reliability, coverage, latency, speed, and sensing accuracy compared to 5G and beyond [1]. With these potential capabilities, 6G can be utilized to realize a wide range of mission-critical applications, e.g., augmented reality (AR), extended reality (XR), virtual reality (VR), robotics and autonomous systems, connected health, holographic or tactile communications, among others.

To realize these heterogeneous applications, traditional orthogonal multiple access (OMA) approaches do not provide an optimal strategy since they can not support the huge number of users or devices owing to inflexible resource allocation [2]. As a result, non-orthogonal multiple access (NOMA) is widely explored in various recent research studies as mobile users can simultaneously share the radio resources, e.g., frequency in the power or code domains [3]. There are considerable benefits which have been achieved using NOMA, such as high spectral

and energy efficiencies, supporting massive connectivity and maintaining fairness among users [4]. Since 6G will combine different emerging technologies, there is still a need to examine the combination between NOMA and other emerging technologies to fully realize the 6G vision and expectations.

Very recently, the use of reconfigurable intelligent surface (RIS) has gained huge attention in the research community as a promising technique to improve the network coverage and connectivity. As such, RIS has been considered as one of potential technologies, together with orthogonal time frequency space (OTFS), for 6G [5]. By adaptive changing the phase and the amplitude of RIS elements, we can achieve the favourable propagation characteristics of wireless channels, thus enhancing the efficiency and throughput of wireless networks [6]. As a result, the combination of NOMA and RIS can naturally increase the network performance. In particular, the channel disparity among users can be enlarged by thoroughly optimizing the placement and reflection coefficients of the RIS so that a higher NOMA gain can be achieved [3].

A wireless channel is a physical medium through which wireless signals propagate between a transmitter and a receiver [7], [8]. Accurate estimation of channel state information (CSI) is crucial in a 6G system, especially in a RIS-NOMA system where scattering, multi-path propagation, power decay, and shadowing effects are highly unpredictable, to mitigate the effects of channel fading, multi-path propagation, and manage interference, hence improving signal quality and data transmission rates [9]. For NOMA systems, achieving a precise CSI is necessary to execute successive interference cancellation (SIC) at each receiver [10]. Moreover, in practice, normally RIS contains a large number of elements, there will be a multitude of channel parameters needed to be estimated, which makes it even more challenging [11].

Quantum technology has given rise to a transformative change in the realm of computing. Quantum computations consist of circuits of parameterized quantum gates that can be trained or optimized by classical optimization methods. Therefore, the quantum machine learning (QML) framework has gained growing attention in many fields, where classical data embedded in quantum bits (qubits) can benefit from

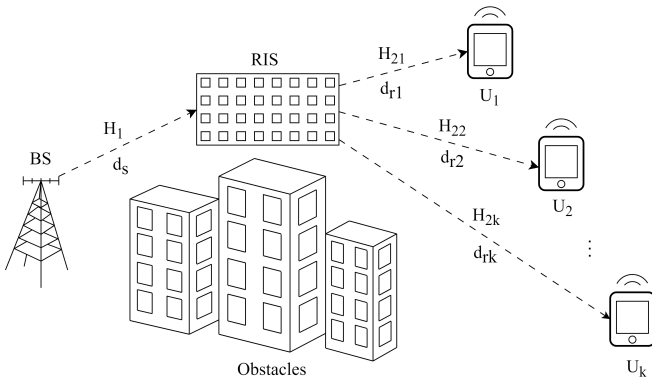


Fig. 1: An illustration of RIS-NOMA assisted 6G downlink communication system.

quantum phenomena to reduce the network size and speed up training time [12]. It is a new paradigm, which can provide considerable computational benefits for many domains, especially in addressing problems of 6G wireless communication, such as signal processing, resource allocation, network traffic optimization, channel estimation, etc [13]. While QML algorithms hold significant potential, their practical application in channel estimation is yet to be explored and is not well-studied in the existing work.

In this work, we propose a QML-based channel estimation method using a convolutional quantum long-short term memory (CNN-QLSTM) model, which takes advantage of CNN and QLSTM, for RIS-NOMA assisted 6G communication system. One of the most significant advantages of the CNN model is its ability to perform automatic feature extraction or feature learning [14]. On the other hand, the vanishing gradient issue in conventional RNN models is addressed by the recurrent neural network (RNN) architecture known as LSTM [15]. The LSTM has shown their ability to capture long-term dependencies in the sequential or time series data [16]. Quantum LSTM (QLSTM), where LSTM is implemented with variational quantum circuits (VQCs), is a framework that has been shown to have faster learning ability and stable convergence than classical counterpart [17]. In this work, We have investigated the performance of the proposed CNN-QLSTM model using root mean square error (RMSE) and mean absolute error (MAE) in a RIS-NOMA aided 6G system.

## II. PROBLEM FORMULATION

In this section, firstly we present a RIS-NOMA aided 6G system model. Then we define the problem in estimating the channel of this system and describe the data preparation for the CNN-QLSTM model. Inspired by the work in [18], we are considering a scenario of the downlink in RIS-aided NOMA system as shown in Fig. 1, where we are considering  $K$  users with  $M$ -antenna are receiving signal from a  $N$ -antenna BS and a RIS with  $L$  reflecting elements. The direct link between the BS to users  $U_k$ ,  $BS \rightarrow U_k$  with  $k \in \{1, 2, \dots, K\}$ , is assumed to be strongly attenuated by obstacles. As a result, each  $U_k$  only receives the signal from the BS with the assistance of

RIS through cascaded channel  $BS \rightarrow RIS \rightarrow U_k$ . At each time step  $t$ ,  $U_k$  is assumed to gradually moving away from the BS with the constant speed  $v$ . We assume that all path links are following Rayleigh fading and the CSI of all cascaded channels are available at the BS.

Given the BS transmit power  $P_t$  and power allocation factor assigned to  $U_k$ , denoted by  $\zeta_k$ , where  $\sum_{k=1}^K \zeta_k^2 = 1$  and  $\zeta_1 < \zeta_2 < \dots < \zeta_K$ , the BS transmits to all users a superposed signal  $x(t) = \sqrt{P_t} \sum_k \zeta_k x_k(t)$  and the received signal at  $U_k$  at time  $t$  is

$$y_k(t) = \sqrt{L_k(t)} \mathbf{H}_{2k}^\dagger(t) \mathbf{\Theta}(t) \mathbf{H}_1(t) \rho \frac{x(t)}{\sqrt{P_t}} + \eta_k(t). \quad (1)$$

In this equation,  $\mathbf{H}_{2k}^\dagger(t) \mathbf{\Theta}(t) \mathbf{H}_1(t)$  refers to the cascaded channel,  $BS \rightarrow RIS \rightarrow U_k$ , at time  $t$  and can be denoted by  $\mathbf{G}_k(t)$ , where  $\mathbf{H}_{2k}(t) \in \mathbb{C}^{L \times M}$  and  $\mathbf{H}_1(t) \in \mathbb{C}^{L \times N}$  represent the channel matrices of the links  $RIS \rightarrow U_k$  and  $BS \rightarrow RIS$  respectively. The  $\mathbf{\Theta}(t) = [\kappa_1 e^{j\varphi_1(t)}, \kappa_2 e^{j\varphi_2(t)}, \dots, \kappa_L e^{j\varphi_L(t)}]^T$  is the diagonal reflection coefficient matrix of RIS, where  $\varphi_l \in [0, 2\pi]$  is the phase shift and  $\kappa_l$  is the amplitude reflection coefficient.  $L_k(t) = L_s L_{rk}(t)$  is the path loss parameter at  $U_k$ , where  $L_s$  and  $L_{rk}(t)$  is the path loss from BS to RIS and from RIS to  $U_k$ , respectively. The path loss is a distance-dependent parameter and is defined as  $L(\hat{d}) = (\hat{d}/d_0)^{-\tau}$  where  $\hat{d}$  is the path link distance,  $d_0$  is reference distance, and the path loss exponent of the environment is defined by  $\tau$  [19]. In equation (1),  $\eta_k(t)$  is the zero mean complex additive white Gaussian noise (AWGN) with variance  $N_0 = 1$  at  $U_k$  and  $\rho = P_t/N_0$  is the transmit signal-to-noise ratio (SNR) with  $\mathbb{E}[\eta_k(t)^2] = N_0$ . After receiving the signal, each user will apply SIC in accordance with the NOMA principle, which allows each user within the system to receive signals of other users. Each user subsequently decodes unwanted signals to attain its desired signal. User with index  $k$  directly decodes its signal  $x_k$  and the corresponding signal-to-interference-plus-noise ratio (SINR) is defined as

$$\varepsilon_k = \frac{|\hat{h}_k|^2 P_t (\zeta_k)^2}{\sum_{i=1}^{k-1} |\hat{h}_i|^2 P_t (\zeta_i)^2 + N_0}, \quad (2)$$

where  $\hat{h}_k = \sqrt{L_k} \mathbf{G}_k$  with  $k = 1, 2, \dots, K$  [20].

### A. Problem Formulation and Data Preparation

In this RIS-NOMA network, we are considering that the channel from  $BS \rightarrow RIS$  remains unchanged, whereas the channels from  $RIS \rightarrow U_k$  are slow time-varying channels due to users moving at a constant speed. Prior knowledge of the cascaded channel gains from  $BS \rightarrow RIS \rightarrow U_k$  is essential for SIC implementation at the receiver side. In this work, we are using received signals at  $U_k$  to estimate the cascaded channel for each user. Employing the dataset generation algorithm in [18], we generate our own dataset for the proposed QML model. In the dataset, we have produced  $\mathbf{S}$  samples where each sample is equivalent to a time step  $t$  in the RIS-NOMA system. The received signal at  $U_k$  denoted by  $\mathbf{Y} \in \mathbb{C}^{S \times K \times MN}$  and the cascaded channel from  $BS \rightarrow RIS \rightarrow U_k$  denoted by

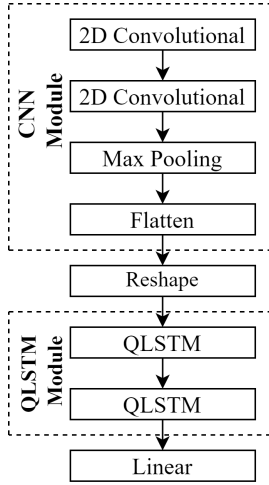


Fig. 2: The structure of CNN-QLSTM model.

$\mathbf{G} \in \mathbb{C}^{S \times K \times MN}$  are generated and served as the input and output respectively for the proposed QML model. The received signal at  $U_k$  represented by  $y_k(t)$  is a complex number. We take its two components: magnitude and phase and merge them into a single dimension. As a result,  $y_k(t) \in \mathbb{R}^{2 \times M \times N}$  and  $\mathbf{Y} \in \mathbb{R}^{S \times K \times 2MN}$ . The entire dataset of  $S$  samples for  $\mathbf{Y}(t)$  and  $\mathbf{G}(t)$  is converted into a time-series sequence with the input time steps  $t_i$  for the proposed CNN-QLSTM model to produce a single-step output. After this conversion, the length of the dataset is altered and is denoted by  $S'$ .

### III. PROPOSED QML MODEL

In this section, a structure of CNN-QLSTM for channel estimation in the RIS-NOMA system is proposed. CNN has been used to capture spatial correlations of the input data. After that, the CNN-derived features are inputted into the QLSTM, which captures the sequential dependencies of the data to predict the output (estimate the cascaded channels). The structure of the proposed QML model is illustrated in Fig. 2.

#### A. CNN Module

CNN is a kind of deep learning model that is commonly used for visual data tasks such as image recognition and classification [21]. Similar to an image, our matrix of the received signal at users including the time steps, the number of users, and the received signals can be regarded as a three-dimensional (3D) image. The CNN module consists of two 2D convolutional (Conv2D) layers, a max pooling (MP) layer and a flatten (FL) layer. The Conv2D layer functions as a feature map, capturing the input data features with filters. The number of filters is denoted by  $N_f$ . Following the second Conv2D, a MP layer with a dimension of  $(p \times p)$  is employed to reduce the dimensionality of the features extracted from CNN. Subsequently, all features are converted to a vector using a FL layer. Prior to inputting them into QLSTM, a reshape (RS) function is applied to match the output size of CNN with the

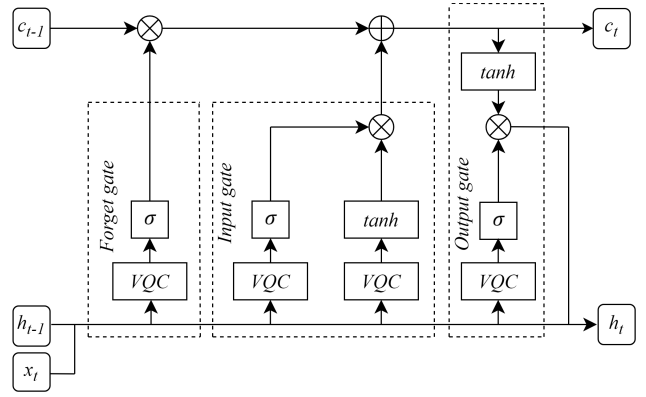


Fig. 3: A QLSTM cell.

input size of QLSTM, which contains the output time steps  $t_o$ .

#### B. QLSTM Module

LSTM is a kind of RNN that has the ability to handle sequences and time-series data. It has been developed to overcome the vanishing gradient problem of RNNs. Inspired by the work in [17], the construction of a QLSTM follows a classical framework but classical neural networks in the LSTM cells are replaced with VQCs, as shown in Fig. 3. The number of the hidden units or QLSTM cells in a layer is denoted by  $N_{hidden}$ . Similar to LSTM, QLSTM consists of 3 main gates. Firstly, the forget gate determines how much information in the previous cell state should be retained or forgotten. Secondly, the input gate decides what new information will be added to the cell state. Thirdly, the output gate decides what information from the cell state should be outputted as the hidden state. In Fig. 3,  $x_t$  is the input,  $h_t$  is the hidden state and  $c_t$  is the cell state at time  $t$ .  $h_{t-1}$  and  $c_{t-1}$  are the hidden state and the cell state at the previous time step  $t-1$ .  $\otimes$  and  $\oplus$  represent element-wise multiplication and addition, respectively.

The structure of VQC used in this paper is shown in Fig. 4, which consists of 3 layers: a) data embedding, b) variational and c) measurement. To embed the classical data into quantum states, we first transform the initial states  $|0\rangle \otimes \dots \otimes |0\rangle$  into unbiased states using Hadamard gates. For each element  $x_i$  in input vector  $\vec{x} = (x_1, x_2, \dots, x_N)$ , firstly we generate angles  $\psi_{i,1} = \arctan(x_i)$  and  $\psi_{i,2} = \arctan(x_i^2)$ . Rotation operators  $R_y$  and  $R_z$  are then respectively applied on  $\psi_{i,1}$  and  $\psi_{i,2}$ . The purpose of taking  $x_i^2$  is to create higher-order terms before inputting the data into the variational layer. In the variational layer, controlled NOT (CNOT) gates are applied to create multi-qubit entanglement and single-qubit rotation gates  $R(\alpha_i, \beta_i, \gamma_i)$  are applied to rotate angles  $\alpha_i, \beta_i$  and  $\gamma_i$  along axes  $x, y$  and  $z$  respectively. We use Pauli-Z gates to measure the states of qubits. The output of the last QLSTM layer is inputted into a Linear layer to map its hidden units to an output of  $N_{f_o}$  features.

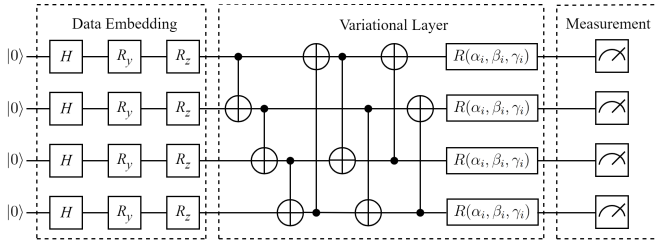


Fig. 4: VQC structure in the QLSTM cell.

#### IV. SIMULATIONS, RESULTS AND DISCUSSIONS

This section describes the simulation settings and discusses the simulation results of channel estimation in RIS-NOMA system using the proposed CNN-QLSTM model.

##### A. Simulation Settings

For the simulation setup, we are considering a single-antenna BS, a RIS with 20 reflecting elements and 2 single-antenna users. The reference distance  $d_0$  is set to 20 m. The distance from BS to RIS is 150 m. The distance from RIS to  $U_1$  and  $U_2$  are respectively 30 m and 40 m. The transmit signal  $x(t)$  and  $\mathbf{H}_1(t)$  follow the distribution  $\mathcal{CN} \sim (1, 0.1)$ .  $\mathbf{H}_{21}(t)$  and  $\mathbf{H}_{22}(t)$  follow  $\mathcal{CN} \sim (4, 1)$  and  $\mathcal{CN} \sim (3, 1)$ , respectively. The dataset is first normalized in the range between 0 and 1 and then divided into 0.8 : 0.2 for training and testing data, respectively. In CNN module, two Conv2D layers have the same hyperparameters:  $N_f = 4$ , kernel size is (3, 3), and padding is 1. The MP layer has  $p = 2$ . In the QLSTM module, two QLSTM layers have  $N_{hidden} = 16$ . The output of the Linear layer is  $N_{fo} = 2$ , which corresponds to the cascaded channel gains of 2 users. The parameters of the proposed model are updated via an Adaptive Gradient Optimizer with a learning rate of 0.05 to minimize the mean square error (MSE) loss function. The configuration of the simulation parameters is provided in Tab. I.

TABLE I: Simulation Parameters.

Parameters	Values
$S'$	2000
$v$	0.1 m
$t_i$	20
$t_o$	1
$L$	20
$\rho$	20 dB
$\kappa_l$	1
$\varphi_l$	$[0.01\pi : 0.02\pi]$
$\tau$ (BS to RIS)	2.2
$\tau$ (RIS to $U_k$ )	2.2
$\eta$	0.3

##### B. Results and Discussions

We have compared the performance of the proposed CNN-QLSTM model with the equivalent classical version i.e. CNN-LSTM using RMSE and MAE metrics. During the training,

both models are trained over 100 epochs using the training dataset and loss curves are shown in Fig. 5. It is observed that the proposed model has a faster convergence and obtained low MSE.

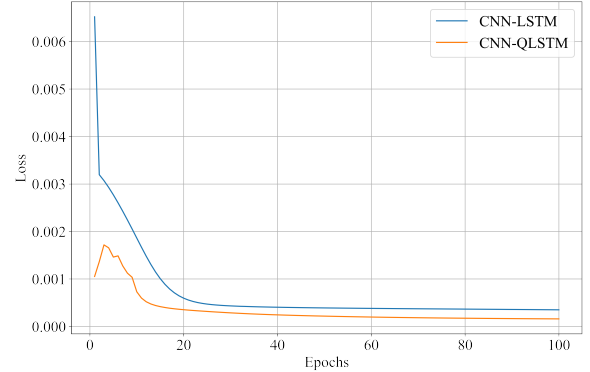


Fig. 5: Loss curve.

We evaluate the performance of our proposed model and equivalent classical version using the test dataset. The CNN-QLSTM model is able to produce better prediction by achieving the least error in terms of RMSE and MAE with the values of 0.006 and 0.005, respectively, for user 1. A similar trend can be observed for user 2. Tab. II shows that the prediction performance of CNN-QLSTM is better than its classical counterpart in terms of RMSE and MAE.

TABLE II: Performance comparison of models.

Model	RMSE		MAE	
	User 1	User 2	User 1	User 2
CNN-LSTM	0.008	0.011	0.007	0.009
CNN-QLSTM	<b>0.006</b>	<b>0.005</b>	<b>0.005</b>	<b>0.004</b>

Fig. 6 and Fig. 7 present the prediction performance of the CNN-QLSTM model on both the training and testing datasets. Here, the dotted line provides a visual indication of data split between training and testing datasets. Fig. 8 shows the prediction performance on the test data for user 2. It is shown that the proposed model keeps track of the target data and variations.

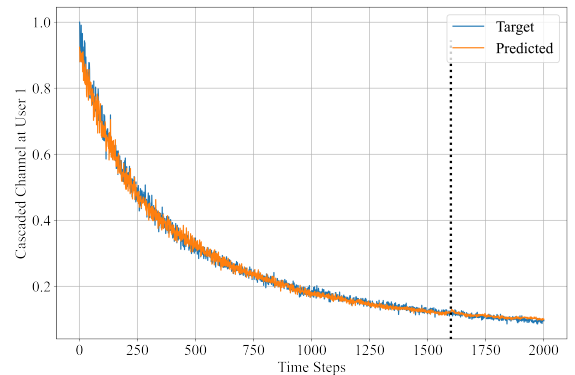


Fig. 6: Prediction performance on user 1.

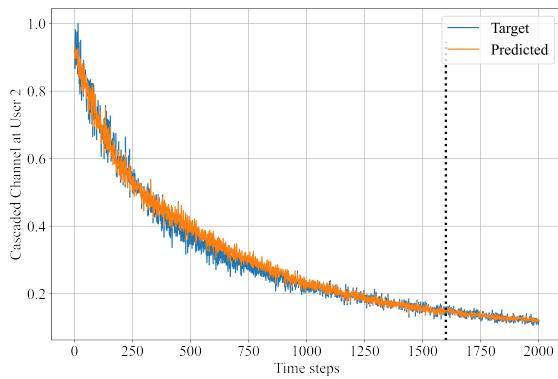


Fig. 7: Prediction performance on user 2.

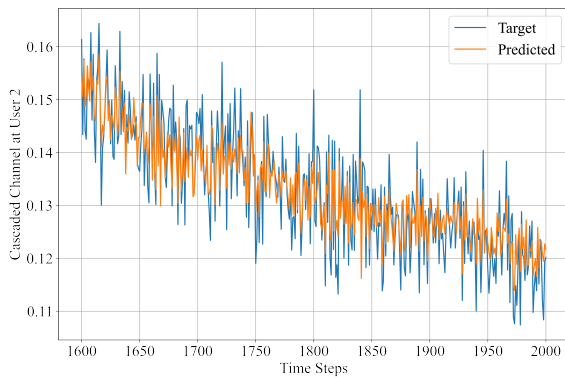


Fig. 8: Prediction performance on user 2 using test data.

## V. CONCLUSION

We propose a CNN-QLSTM model for channel prediction in RIS-aided 6G NOMA system. Our results demonstrate that the proposed model has better ability to reduce the error and obtain faster convergence during the training phase. Moreover, the CNN-QLSTM model has a better prediction on the testing data compared to CNN-LSTM based on RMSE and MAE. Our paper demonstrates the potential use of quantum machine learning in channel estimation tasks. However, requires further investigation to optimize the model's performance. In future, different structures of variational quantum circuits will be explored to exploit the advantages of the quantum machine learning in the learning capability and computational speed.

## ACKNOWLEDGEMENTS

This work was supported in part by the Canada Excellence Research Chair (CERC) Program CERC-2022-00109 and in part by the Canada Research Chair Program CRC-2022-00187. The authors would also like to thanks Xanadu for providing support with PennyLane.

## REFERENCES

[1] C.-X. Wang, X. You, X. Gao, X. Zhu, Z. Li, C. Zhang, H. Wang, Y. Huang, Y. Chen, H. Haas, J. S. Thompson, E. G. Larsson, M. D. Renzo, W. Tong, P. Zhu, X. Shen, H. V. Poor, and L. Hanzo, "On the

Road to 6G: Visions, Requirements, Key Technologies, and Testbeds," *IEEE Commun. Surveys Tuts.*, vol. 25, no. 2, pp. 905–974, Apr. 2023.

[2] Y. Liu, S. Zhang, X. Mu, Z. Ding, R. Schober, N. Al-Dhahir, E. Hossain, and X. Shen, "Evolution of NOMA Toward Next Generation Multiple Access (NGMA) for 6G," *IEEE J. Sel. Areas Commun.*, vol. 40, no. 4, pp. 1037–1071, Apr. 2022.

[3] Z. Ding, X. Lei, G. K. Karagiannidis, R. Schober, J. Yuan, and V. K. Bhargava, "A Survey on Non-Orthogonal Multiple Access for 5G Networks: Research Challenges and Future trends," *IEEE J. Sel. Areas Commun.*, vol. 35, no. 10, pp. 2181–2195, Oct. 2017.

[4] B. Zheng, Q. Wu, and R. Zhang, "Intelligent Reflecting Surface-Assisted Multiple Access With user pairing: NOMA or OMA?" *IEEE Commun. Lett.*, vol. 24, no. 4, pp. 753–757, Apr. 2020.

[5] J. Zuo, Y. Liu, Z. Qin, and N. Al-Dhahir, "Resource Allocation in Intelligent Reflecting Surface Assisted NOMA Systems," *IEEE Trans. Commun.*, vol. 68, no. 11, pp. 7170–7183, Nov. 2020.

[6] Y. Liu, X. Liu, X. Mu, T. Hou, J. Xu, M. Di Renzo, and N. Al-Dhahir, "Reconfigurable Intelligent Surfaces: Principles and Opportunities," *IEEE Commun. Surveys Tuts.*, vol. 23, no. 3, pp. 1546–1577, 3rd Quart. 2021.

[7] Y. Zhang, R. He, B. Ai, M. Yang, R. Chen, C. Wang, Z. Zhang, and Z. Zhong, "Generative Adversarial Networks Based Digital Twin Channel Modeling for Intelligent Communication Networks," *China Communications*, vol. 20, no. 8, pp. 32–43, Aug. 2023.

[8] C. Luo, J. Ji, Q. Wang, X. Chen, and P. Li, "Channel State Information Prediction for 5G Wireless Communications: A Deep Learning Approach," *IEEE Trans. Netw. Sci. Eng.*, vol. 7, no. 1, pp. 227–236, Jan.–Mar. 2020.

[9] K. Weththasinghe, B. Jayawickrama, and Y. He, "Machine Learning-Based Channel Estimation for 5G New Radio," *IEEE Wireless Commun. Lett.*, vol. 13, no. 4, pp. 1133–1137, Apr. 2024.

[10] G. Yang, X. Xu, Y.-C. Liang, and M. D. Renzo, "Reconfigurable Intelligent Surface-Assisted Non-Orthogonal Multiple Access," *IEEE Trans. Wireless Commun.*, vol. 20, no. 5, pp. 3137–3151, May 2021.

[11] W. Shen, Z. Qin, and A. Nallanathan, "Deep Learning for Super-Resolution Channel Estimation in Reconfigurable Intelligent Surface Aided Systems," *IEEE Trans. Commun.*, vol. 71, no. 3, pp. 1491–1503, Mar. 2023.

[12] T. M. Khan and A. Robles-Kelly, "Machine Learning: Quantum vs Classical," *IEEE Access*, vol. 8, pp. 219 275–219 294, Dec. 2020.

[13] S. J. Nawaz, S. K. Sharma, S. Wyne, M. N. Patwary, and M. Asaduzaman, "Quantum Machine Learning for 6G Communication Networks: State-of-the-Art and Vision for the Future," *IEEE Access*, vol. 7, pp. 46 317–46 350, Apr. 2019.

[14] J. B. Thomas, S. G. Chaudhari, S. K. V., and N. K. Verma, "CNN-Based Transformer Model for Fault Detection in Power System Networks," *IEEE Trans. Instrum. Meas.*, vol. 72, pp. 1–10, Jan. 2023.

[15] O. Rubasinghe, X. Zhang, T. K. Chau, Y. H. Chow, T. Fernando, and H. H.-C. Iu, "A Novel Sequence to Sequence Data Modelling Based CNN-LSTM Algorithm for Three Years Ahead Monthly Peak Load Forecasting," *IEEE Trans. Power Syst.*, vol. 39, no. 1, pp. 1932–1947, Jan. 2024.

[16] Z. Ali, A. Muhammad, A. S. Al-Shamayleh, K. N. Qureshi, W. Al-ragwaf, and A. Akhuzada, "Enhancing Performance of Movie Recommendations Using LSTM With Meta Path Analysis," *IEEE Access*, vol. 11, pp. 119 017–119 032, Oct. 2023.

[17] S. Y.-C. Chen, S. Yoo, and Y.-L. L. Fang, "Quantum Long Short-Term Memory," in *Proc. of the IEEE Int. Conf. Acoust., Speech, Signal Process.*, May 2022, pp. 8622–8626.

[18] C. Nguyen, T. M. Hoang, and A. A. Cheema, "Channel Estimation Using CNN-LSTM in RIS-NOMA Assisted 6G Network," *IEEE Trans. Mach. Learn. Commun. Netw.*, vol. 1, pp. 43–60, May 2023.

[19] Y. Han, N. Li, Y. Liu, T. Zhang, and X. Tao, "Artificial Noise Aided Secure NOMA Communications in STAR-RIS Networks," *IEEE Wireless Commun. Lett.*, vol. 11, no. 6, pp. 1191–1195, Jun. 2022.

[20] Y. Pei, X. Yue, W. Yi, Y. Liu, X. Li, and Z. Ding, "Secrecy Outage Probability Analysis for Downlink RIS-NOMA Networks With On-Off Control," *IEEE Trans. Veh. Technol.*, vol. 72, no. 9, pp. 11 772–11 786, Sep. 2023.

[21] Z.-Q. Zhao, P. Zheng, S.-T. Xu, and X. Wu, "Object Detection With Deep Learning: A Review," *IEEE Trans. Neural Netw. Learn. Syst.*, vol. 30, no. 11, pp. 3212–3232, Nov. 2019.